Paper presentation

Soham
04 Jan 2025

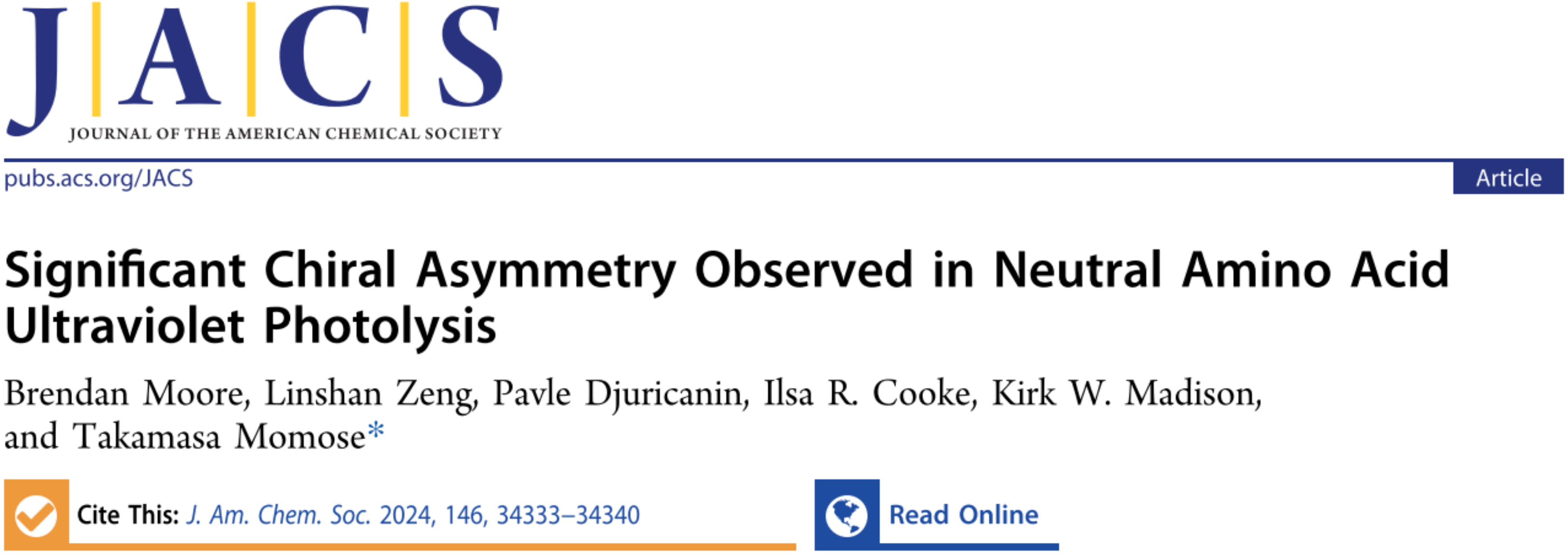

JACS
JOURNAL OF THE AMERICAN CHEMICAL SOCIETY
pubs.acs.org/JACS
Article

Significant Chiral Asymmetry Observed in Neutral Amino Acid Ultraviolet Photolysis

Brendan Moore, Linshan Zeng, Pavle Djuricanin, Ilsa R. Cooke, Kirk W. Madison, and Takamasa Momose*

Cite This: *J. Am. Chem. Soc.* 2024, 146, 34333–34340

Read Online

Department of Chemistry, The University of British Columbia, Vancouver, Canada

Department of Physics and Astronomy, The University of British Columbia, Vancouver, Canada

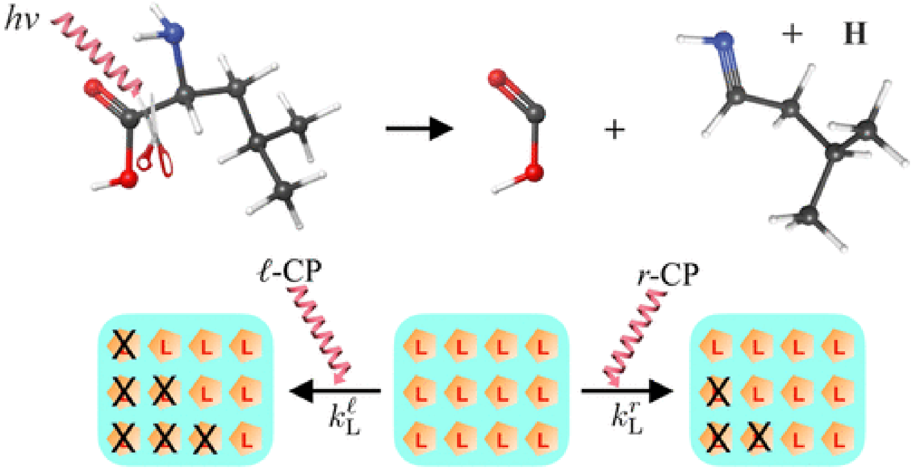

Background

Letter | Published: 18 September 1997

Isotopic evidence for extraterrestrial non- racemic amino acids in the Murchison meteorite

M. H. Engel & S. A. Macko

Nature **389**, 265–268 (1997) | Cite this article

3813 Accesses | **402** Citations | **23** Altmetric | Metrics

REPORTS

Enantiomeric Excesses in Meteoritic Amino Acids

JOHN R. CRONIN AND SANDRA PIZZARELLO Authors Info & Affiliations

SCIENCE • 14 Feb 1997 • Vol 275, Issue 5302 • pp. 951-955 • DOI: 10.1126/science.275.5302.951

1,092 10

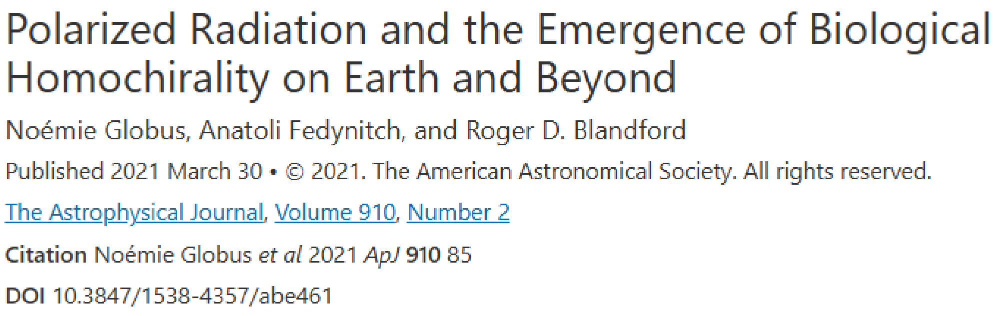

Polarized Radiation and the Emergence of Biological Homochirality on Earth and Beyond

Noémie Globus, Anatoli Fedynitch, and Roger D. Blandford

Published 2021 March 30 • © 2021. The American Astronomical Society. All rights reserved.

The Astrophysical Journal, Volume 910, Number 2

Citation Noémie Globus *et al* 2021 *ApJ* **910** 85

DOI 10.3847/1538-4357/abe461

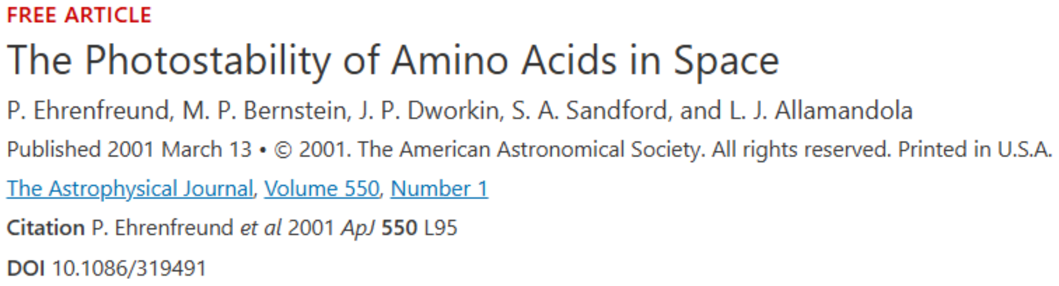

FREE ARTICLE

The Photostability of Amino Acids in Space

P. Ehrenfreund, M. P. Bernstein, J. P. Dworkin, S. A. Sandford, and L. J. Allamandola

Published 2001 March 13 • © 2001. The American Astronomical Society. All rights reserved. Printed in U.S.A.

The Astrophysical Journal, Volume 550, Number 1

Citation P. Ehrenfreund *et al* 2001 *ApJ* **550** L95

DOI 10.1086/319491

Background

Communication | Full Access

Photonenergy-Controlled Symmetry Breaking with Circularly Polarized Light†

Dr. Cornelia Meinert, Dr. Søren V. Hoffmann, Dr. Patrick Cassam-Chenaï, Dr. Amanda C. Evans, Chaitanya Giri, Dr. Laurent Nahon, Prof. Dr. Uwe J. Meierhenrich

First published: 13 November 2013 | https://doi.org/10.1002/anie.201307855 | Citations: 102

On the origins of life's homochirality: Inducing enantiomeric excess with spin-polarized electrons

S. Furkan Ozturk and Dimitar D. Sasselov Authors Info & Affiliations

Edited by Ron Naaman, Weizmann Institute of Science, Rehovot, Israel; received March 21, 2022; accepted May 5, 2022 by Editorial Board Member Joanna Aizenberg

July 5, 2022 | 119 (28) e2204765119 | https://doi.org/10.1073/pnas.2204765119

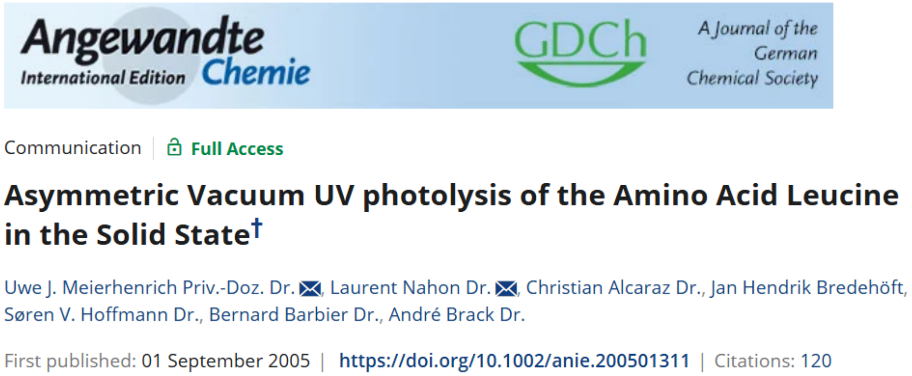

Communication | Full Access

Asymmetric Vacuum UV photolysis of the Amino Acid Leucine in the Solid State†

Uwe J. Meierhenrich Priv.-Doz. Dr., Laurent Nahon Dr., Christian Alcaraz Dr., Jan Hendrik Bredehöft, Søren V. Hoffmann Dr., Bernard Barbier Dr., André Brack Dr.

First published: 01 September 2005 | https://doi.org/10.1002/anie.200501311 | Citations: 120

COMMUNICATION | December 1, 1998

Is Arginine Zwitterionic or Neutral in the Gas Phase? Results from IR Cavity Ringdown Spectroscopy

C. J. Chapo, J. B. Paul, R. A. Provencal, K. Roth, and R. J. Saykally

Motivation

parahydrogen (pH_2) matrix isolation spectroscopy

- molecules are isolated in cold, inert crystals
- solid parahydrogen offers an unparalleled cage-free environment
- amino acids in interstellar space predominantly exist in their nonzwitterionic “neutral” form while in the gas phase or adsorbed to grain surfaces at low temperature.

- investigate asymmetric photolysis of neutral amino acids to further substantiate the likelihood the extraterrestrial origin hypothesis

Key findings

- evidence of significant asymmetry in the chiral-destroying dissociation rate of leucine’s lowest energy neutral form conformer induced by circularly polarized photons at 213 nm
- The observed anisotropy factor for the lowest energy conformer of leucine was remarkably large, reaching 0.1–a factor of 13 times larger than observed for zwitterionic leucine in solid films, and nearly 40 times greater than the anisotropy reported in the electronic absorption spectrum of gas-phase leucine ensembles at room temperature.

Instrumentation

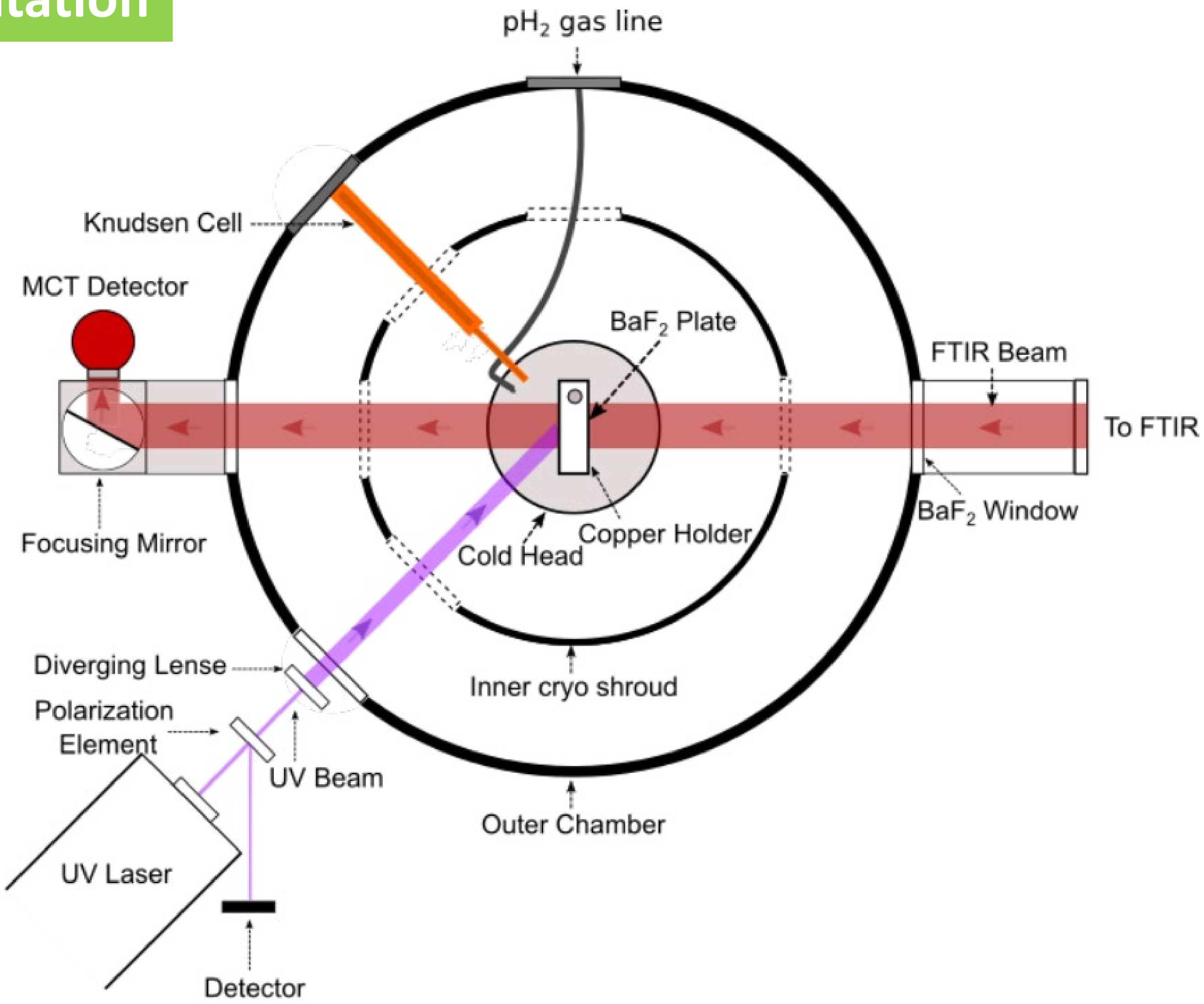

Schematic of the matrix isolation vacuum chamber, the deposition line and Knudsen cell setup, the UV irradiation geometry, as well as the geometry of the infrared light detection by the liquid nitrogen-cooled MCT detector.

Results

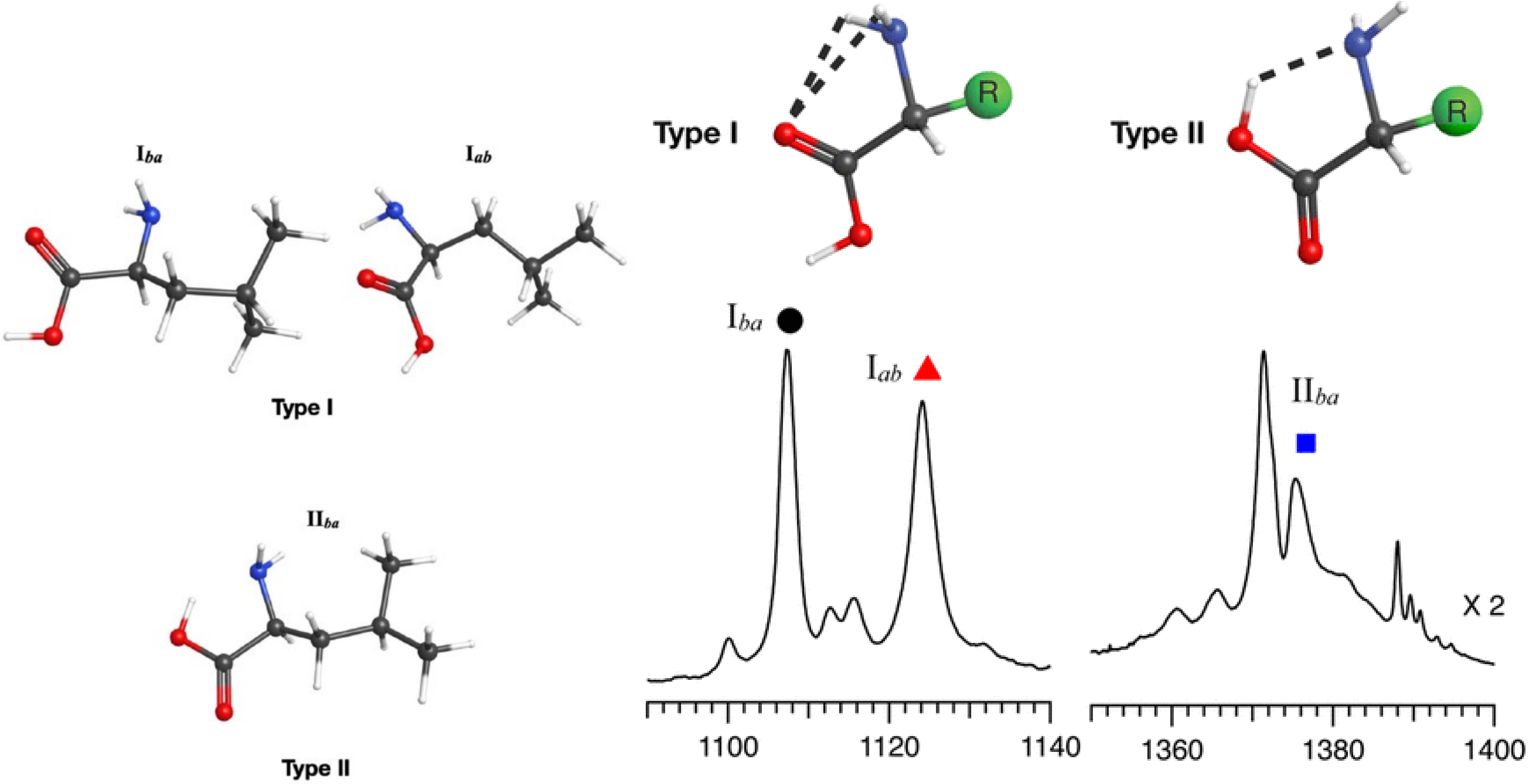

Figure 1. FTIR spectra of leucine in a pH_2 matrix. The peaks marked by a black filled circle, red filled triangle, and blue filled square are the conformers I_{ba}, I_{ab}, and II_{ba} respectively. The structures of Type I and II leucine conformers are also shown, where R represents the $CH_2CH(CH_3)_2$ unit of leucine.

Results

Scheme 1. Photodissociation of L-Leucine by 213 or 193 nm Photons

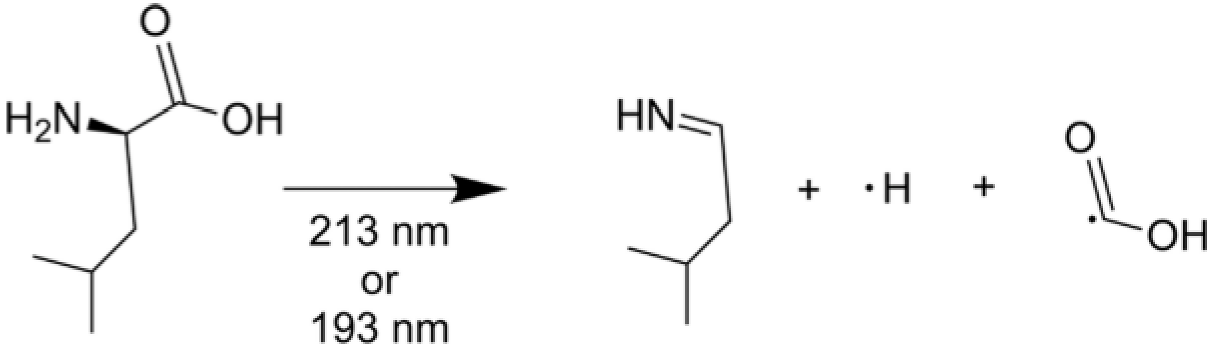

Results

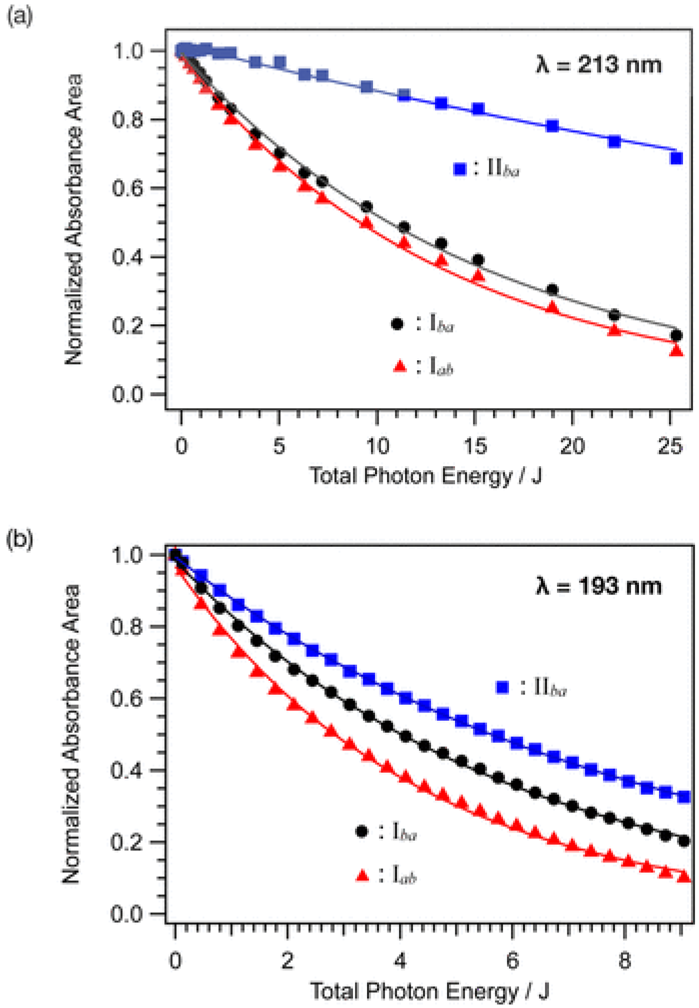

Figure 2. The decay of leucine infrared absorbance upon irradiation. (a) 213 nm irradiation. (b) 193 nm irradiation. The plots shown here represent the decay of D-leucine absorbance under l-CPL irradiation as examples. The *x*-axis of each panel shows the total irradiation energy, the laser pulse energy (in J) multiplied by the number of pulses which is proportional to the accumulated number of irradiated UV photons. Curve fitting by a single exponential function, $\exp(-kx)$, is also shown for each peak, where k represents the decay rate constant due to the photodissociation.

Results

Fig. S2. Relation between the observed decay rate constants, k, and the anisotropy factors g.

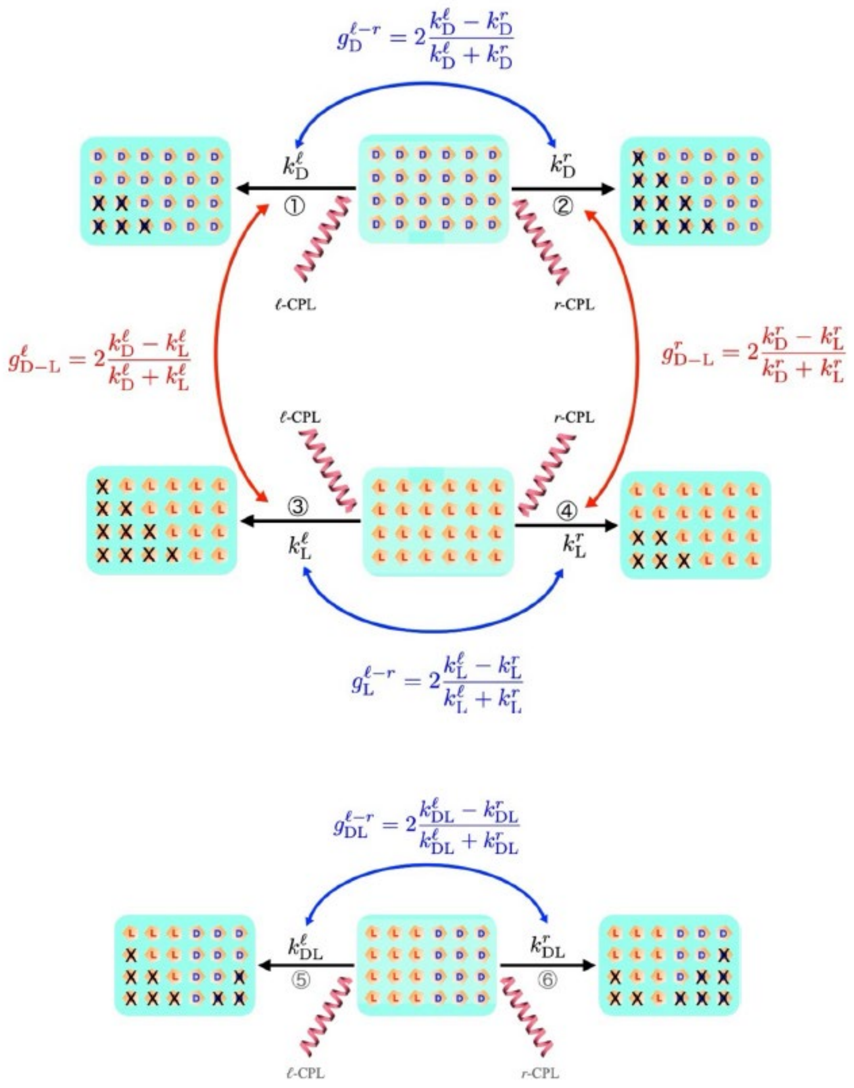

Results

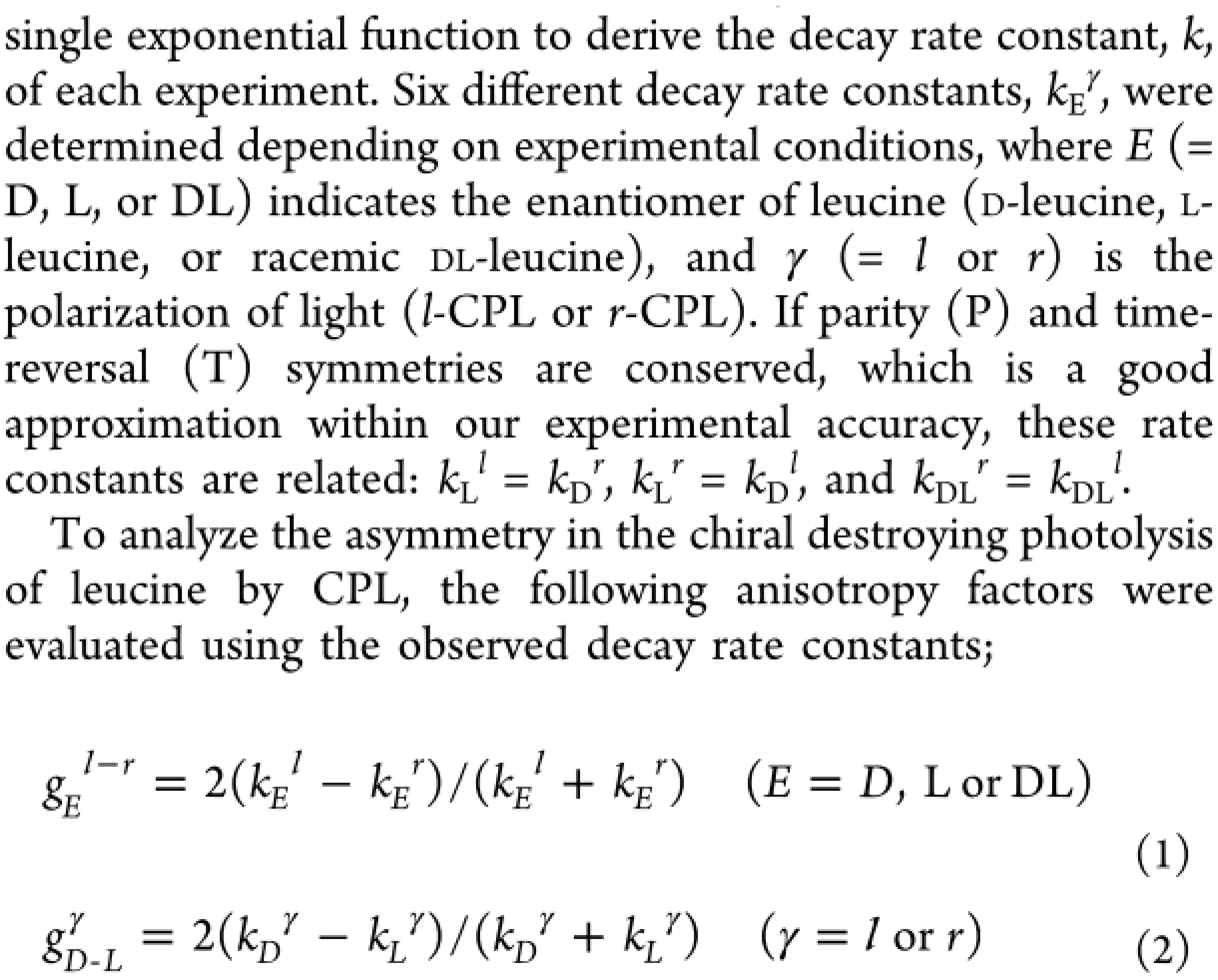

single exponential function to derive the decay rate constant, k, of each experiment. Six different decay rate constants, k_E^{γ}, were determined depending on experimental conditions, where E (= D, L, or DL) indicates the enantiomer of leucine (D-leucine, L-leucine, or racemic DL-leucine), and γ (= l or r) is the polarization of light (l-CPL or r-CPL). If parity (P) and time-reversal (T) symmetries are conserved, which is a good approximation within our experimental accuracy, these rate constants are related: $k_L^{\,l} = k_D^{\,r}$, $k_L^{\,r} = k_D^{\,l}$, and $k_{DL}^{\,r} = k_{DL}^{\,l}$.

To analyze the asymmetry in the chiral destroying photolysis of leucine by CPL, the following anisotropy factors were evaluated using the observed decay rate constants;

$$g_E^{\,l-r} = 2(k_E^{\,l} - k_E^{\,r})/(k_E^{\,l} + k_E^{\,r}) \quad (E = D,\ \mathrm{L\ or\ DL}) \tag{1}$$

$$g_{D\text{-}L}^{\gamma} = 2(k_D^{\,\gamma} - k_L^{\,\gamma})/(k_D^{\,\gamma} + k_L^{\,\gamma}) \quad (\gamma = l \text{ or } r) \tag{2}$$

Results

Table 1. Anisotropy Factors of the 213 nm (a) and 193 nm (b) Photolysis of Leucine Type I and II Conformers[a]

(a) 213 nm								
conformer	transition (cm^{-1})	$g_{D}^{l\text{-}r}$	$g_{L}^{l\text{-}r}$	$\overline{g}^{l\text{-}r}$	$g_{D\text{-}L}^{l}$	$g_{D\text{-}L}^{r}$	$\overline{g}_{D\text{-}L}$	$g_{DL}^{l\text{-}r}$
I_{ba}	1107.2	−0.09(6)	0.12(5)	−0.11(4)	−0.06(4)	0.14(7)	−0.08(4)	−0.02(4)
I_{ab}	1123.9	−0.06(5)	0.15(5)	−0.10(3)	−0.08(4)	0.12(6)	−0.09(3)	−0.02(4)
II_{ba}	1375.1	0.04(6)	0.13(12)	−0.01(7)	0.04(4)	0.13(13)	−0.02(7)	−0.03(13)
(b) 193 nm								
conformer	transition (cm^{-1})	$g_{D}^{l\text{-}r}$	$g_{L}^{l\text{-}r}$	$\overline{g}^{l\text{-}r}$	$g_{D\text{-}L}^{l}$	$g_{D\text{-}L}^{r}$	$\overline{g}_{D\text{-}L}$	$g_{DL}^{l\text{-}r}$
I_{ba}	1107.2	−0.032(21)	0.011(20)	−0.015(12)	−0.034(26)	−0.024(16)	−0.009(16)	–
I_{ab}	1123.9	−0.025(12)	−0.003(12)	−0.020(14)	−0.008(26)	0.012(6)	−0.012(13)	–
II_{ba}	1375.1	−0.022(16)	−0.005(25)	−0.020(15)	−0.005(25)	−0.039(34)	−0.016(21)	–

[a] Values in parentheses indicate the standard error (1σ) for the last digit. The weighted average of $g_{D}^{l\text{-}r}$ and $-g_{L}^{l\text{-}r}$ is shown as $\overline{g}^{l\text{-}r}$, while that of $g_{D\text{-}L}^{l}$ and $-g_{D\text{-}L}^{r}$ is shown as $\overline{g}_{D\text{-}L}$.

Since $g_{D}^{l\text{-}r}$ and $g_{L}^{l\text{-}r}$ are expected to be the same magnitude with opposite sign, we computed the inverse-variance-weighted average of $g_{D}^{l\text{-}r}$ and$-g_{L}^{l\text{-}r}$, which is shown as $\overline{g}^{l-r}$ in Table 1. A similar relationship is expected for $g_{D\text{-}L}^{l}$ and $g_{D\text{-}L}^{r}$, and the weighted average of $g_{D\text{-}L}^{l}$ and $-g_{D\text{-}L}^{r}$ is shown as $\overline{g}_{D-L}$ in Table 1. The definition of $\overline{g}^{l-r}$ and $\overline{g}_{D-L}$ is such that both values are negative if L-leucine is destroyed more efficiently by *l*-CPL than *r*-CPL. The values of $\overline{g}^{l-r}$ and $\overline{g}_{D-L}$ are expected to be the same within our experimental accuracy. Note that the magnitude of the mean values of $g_{D}^{l\text{-}r}$ and $g_{L}^{l\text{-}r}$, as well as those of $g_{D\text{-}L}^{l}$ and $g_{D\text{-}L}^{r}$, match within a 1σ error range. The observed variation in the mean values is still attributed to statistical errors, and increasing the number of measurements would likely reduce this variation.

Results

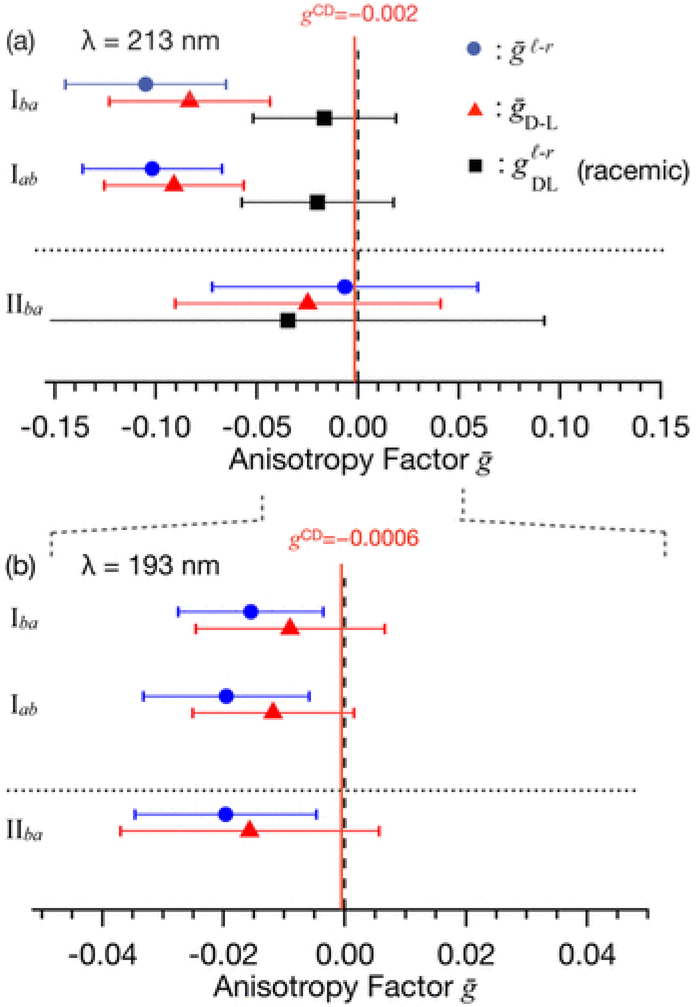

Figure 3. Anisotropy factors determined from the UV photolysis of neutral leucine. (a) 213 nm irradiation. (b) 193 nm irradiation. Blue circles (blue solid circle symbol) represent $\overline{g}^{l-r}$, the weighted average of $g_D{}^{l-r}$ and $-g_L{}^{l-r}$, for enantiopure leucine. Red triangles (red solid triangle symbol) represent $\overline{g}_{D-L}$ (the weighted average of $g_{D-L}{}^{l}$ and $-g_{D-L}{}^{r}$, for enantiopure leucine. Black squares (■) represent $g_{DL}{}^{l-r}$ of racemic DL-leucine. Error bars show the 1σ uncertainty. The broken vertical line in each panel represents $g = 0.0$, while the solid red line indicates the gas phase asymmetry factor.

Comparison with circular dichroism

- The negative anisotropy factor for d-leucine and the positive anisotropy factor for l-leucine at 213 nm are in the same direction as our photolysis observations
- the magnitude of the CD anisotropy is tiny in comparison, +0.002139 and −0.00191 for l- and d-leucine, respectively, at 213 nm

- pH2 crystal environment could have shifted the absorption peak wavelengths
- matrix orientation (orientational average of $\langle \cos^2\theta \rangle$ is 1/3)
- overlapping CD peaks from different conformers tend to cancel out each other, resulting in markedly subdued overall CD magnitude

Results

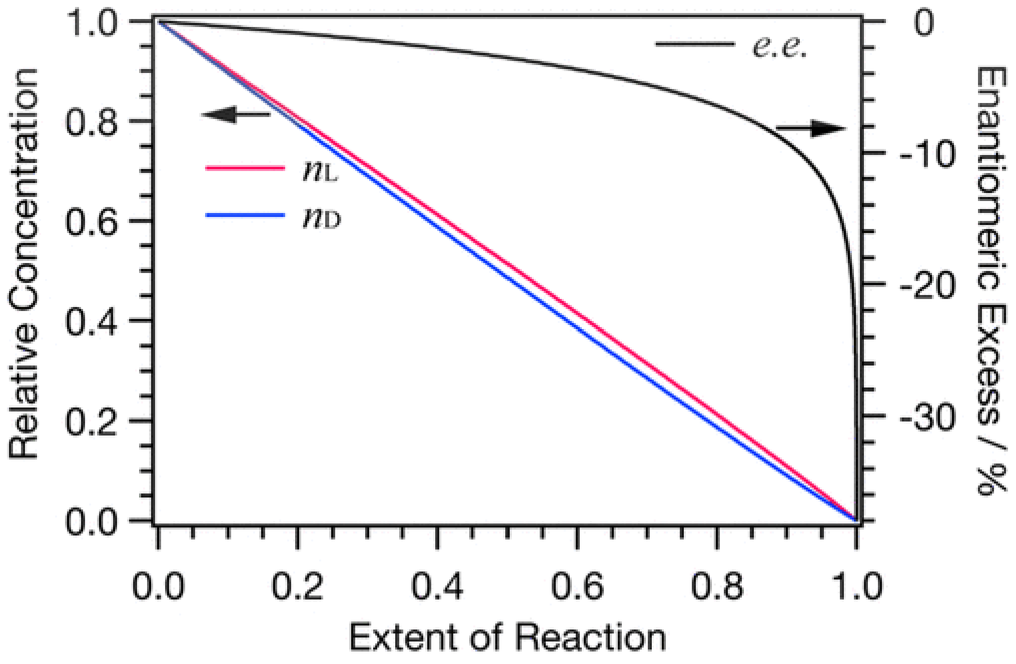

Figure 4. Simulated changes of the concentration and the enantiomeric excess as a function of the extent of reaction. Blue line n_D: Simulated changes in the concentration of D-leucine relative to the original concentrations ($n_L(0) = n_D(0) =1$) as a function of the extent of reaction for the case of $g = -0.08$ and irradiated by *r*-CPL. Red line n_L: That of L-leucine. Black line: The enantiomeric excess, defined as $(n_D - n_L)/(n_D + n_L) \times 100$) The negative enantiomeric excess indicates the enrichment of L-leucine via *r*-CPL.

Conclusion

- strong asymmetry favoring the destruction of d-leucine (or the enrichment of l-leucine) by r-CPL, was confirmed for the photolysis of Type I leucine by 213 nm light.
- observation of asymmetry of individual conformers, precisely analyze the individual contributions of conformers to the overall asymmetry in the photolysis dynamics.